Control of metastatic niche formation by targeting APBA3/Mint3 in inflammatory monocytes

Toshiro Hara[a], Hiroki J. Nakaoka[a,b], Tetsuro Hayashi[b], Kouhei Mimura[a], Daisuke Hoshino[a], Masahiro Inoue[c], Fumitaka Nagamura[d], Yoshinori Murakami[b], Motoharu Seiki[a,e], and Takeharu Sakamoto[a,b,1]

[a]Division of Cancer Cell Research, Institute of Medical Science, The University of Tokyo, Minato-ku, Tokyo 108-8639, Japan; [b]Division of Molecular Pathology, Institute of Medical Science, The University of Tokyo, Minato-ku, Tokyo 108-8639, Japan; [c]Department of Biochemistry, Osaka Medical Center for Cancer and Cardiovascular Diseases, Osaka 541-8567, Japan; [d]Division of Advanced Medicine Promotion, Institute of Medical Science, The University of Tokyo, Minato-ku, Tokyo 108-8639, Japan; and [e]Faculty of Medicine, Institute of Medical, Pharmaceutical and Health Sciences, Kanazawa University, Kanazawa, Ishikawa 920-0942, Japan

Edited by Zena Werb, University of California, San Francisco, CA, and approved April 20, 2017 (received for review February 27, 2017)

Cancer metastasis is intricately orchestrated by both cancer and normal cells, such as endothelial cells and macrophages. Monocytes/macrophages, which are often co-opted by cancer cells and promote tumor malignancy, acquire more than half of their energy from glycolysis even during normoxic conditions. This glycolytic activity is maintained during normoxia by the functions of hypoxia inducible factor 1 (HIF-1) and its activator APBA3. The mechanism by which APBA3 inhibition partially suppresses macrophage function and affects cancer metastasis is of interest in view of avoidance of the adverse effects of complete suppression of macrophage function during therapy. Here, we report that APBA3-deficient mice show reduced metastasis, with no apparent effect on primary tumor growth. APBA3 deficiency in inflammatory monocytes, which strongly express the chemokine receptor CCR2 and are recruited toward chemokine CCL2 from metastatic sites, hampers glycolysis-dependent chemotaxis of cells toward metastatic sites and inhibits VEGFA expression, similar to the effects observed with HIF-1 deficiency. Host APBA3 induces VEGFA-mediated E-selectin expression in the endothelial cells of target organs, thereby promoting extravasation of cancer cells and micrometastasis formation. Administration of E-selectin–neutralizing antibody also abolished host APBA3-mediated metastatic formation. Thus, targeting APBA3 is useful for controlling metastatic niche formation by inflammatory monocytes.

APBA3/Mint3 | macrophage | metastasis

Cancer metastasis comprises multiple processes of neoplastic progression, termed the "invasion–metastasis cascade" (1, 2). Thousands of circulating tumor cells (CTCs) can be released from invasive primary tumors; however, most patients develop only a few metastases, suggesting that metastatic initiation processes (such as extravasation and colonization at distant organs) are quite inefficient but key for controlling metastatic cancer diseases. Unlike at primary sites, single or small groups of disseminated CTCs encounter large numbers of normal cells in their new environments, which determines their survival and metastatic efficiency, as shown by studies with genetically engineered mouse models (3–5).

Macrophages are myeloid cells that are co-opted essentially to foster tumor progression and metastasis. The functions of tumor-associated macrophages include angiogenesis, suppression of antitumor immune responses, chemoresistance, and metastasis; these are considered novel targets for cancer therapy (6–10). Monocytes (i.e., macrophage precursors) are characterized by the surface molecules CD11b and CD115, and comprise at least two subsets: Gr-1^{+}(Ly-6C^{high})CCR2^{+}CX3CR1^{low} inflammatory monocytes (IMs) and Gr-1^{low}(Ly-6C^{low})CCR2^{low}CX3CR1^{high} resident monocytes (RMs) (11). Their recruitment from the bone marrow (BM) to peripheral tissues is mediated mainly by chemokine–chemokine receptor complexes such as the CCL2/CCR2 system (12, 13). Even in metastatic cascades, the CCL2–CCR2 axis is a key pathway for IM recruitment, which in turn promotes tumor colonization and metastasis by secreting VEGFA (14, 15). Moreover, the prevalence of IMs in the peripheral blood, as induced by the CCL2–CCR2 axis, correlates with liver metastasis, adverse outcome, and shorter patient survival in pancreatic cancer (16). Although the cellular landscapes involved in metastasis formation have been well-described with macrophage lineages, the molecular mechanisms underlying metastasis (such as with metabolic fueling and metastasis-associated monocytes/macrophages) remain unclear.

Macrophages are unique in that they produce ATP mainly by glycolysis, rather than by mitochondrial oxidative phosphorylation, during normoxic conditions, because hypoxia-inducible factor 1 (HIF-1), which is usually activated during hypoxia, retains its activity even during normoxia in macrophages (17–19). This constitutive activation is caused by suppression of factor inhibiting HIF-1 (FIH-1) (20, 21), which inhibits HIF-1 transcriptional activity in an oxygen-dependent manner (18). This effect is abrogated by APBA3/Mint3, enhancing HIF-1 activity in macrophages (20–22). Indeed, APBA3 deficiency diminishes HIF-1 activity and the expression of HIF-1 target genes during normoxia but retains the HIF-1 response to hypoxia in macrophages.

Approximately 60% of total ATP production in macrophages during normoxia is APBA3-dependent (20, 22). APBA3-deficient (*Apba3*$^{-/-}$) mice are apparently normal and fertile. However, they are resistant to lipopolysaccharide-induced septic shock, due to specific defects in macrophages. Moreover, recruitment of macrophages to acute inflammatory sites is inhibited, although

Significance

Metastasis complicates cancer treatment. This process is intricately orchestrated by both cancer and normal cells. Thus, new antimetastasis drugs targeting normal cells that interact with cancer cells constitutes a promising approach, as long as body homeostasis is unaffected. Here, we focused on a unique feature of metastasis-promoting monocytes/macrophages: their dependence on aerobic glycolysis for energy production. APBA3 promotes aerobic glycolysis by activating HIF-1 in macrophages. APBA3 depletion decreases ATP production by approximately 60% in macrophages without affecting other cells. We show that depletion of APBA3 in monocytes suppresses their recruitment to the metastatic niche and E-selectin induction in endothelial cells, resulting in metastasis inhibition. Thus, targeting APBA3 may be useful for preventing metastasis, with few side effects.

Author contributions: T. Hara, M.I., F.N., Y.M., M.S., and T.S. designed research; T. Hara, H.J.N., T. Hayashi, K.M., and D.H. performed research; T. Hara and H.J.N. analyzed data; and T. Hara, M.S., and T.S. wrote the paper.

The authors declare no conflict of interest.

This article is a PNAS Direct Submission.

Freely available online through the PNAS open access option.

[1]To whom correspondence should be addressed. Email: t-saka@ims.u-tokyo.ac.jp.

This article contains supporting information online at www.pnas.org/lookup/suppl/doi:10.1073/pnas.1703171114/-/DCSupplemental.

the number of macrophages is not different in *Apba3*$^{-/-}$ mice. Although macrophage inhibition may suppress metastasis, their complete suppression is unfavorable because they are crucial for maintaining body homeostasis. The mechanism by which APBA3 inhibition partially suppresses macrophage function and affects cancer metastasis is therefore of interest.

Here, using *Apba3*$^{-/-}$ and the corresponding conditional knockout mice, we show that APBA3 depletion in monocytes/macrophages contributes to metastasis suppression. APBA3-dependent VEGFA expression in monocytes/macrophages recruited to the metastatic niche induces E-selectin expression in the endothelial cells of target organs in which cancer cells are trapped, extravasate, and form micrometastases.

Results

Host APBA3 Supports Metastasis Formation. Extravasation and colonization are key processes required for cancer cell metastasis. To test whether APBA3 expression in the tumor microenvironment could directly impact these processes, we inoculated a well-established metastatic mouse cell line, B16F10 melanoma cells, directly into the lateral tail vein of mice, with or without APBA3 deficiency. *Apba3*$^{-/-}$ mice showed decreased lung metastasis, as determined by visually counting metastatic foci with melanin pigmentation in the lungs, which resulted in prolonged survival (Fig. 1 *A* and *B*). In agreement with these findings, we i.v. injected other mouse cell lines, including Lewis lung carcinoma (LLC) cells and 4T1 breast cancer cells, which established fewer metastatic foci and exhibited longer survival in *Apba3*$^{-/-}$ mice than in WT mice (Fig. 1 *C*–*F*). Thus, these data suggested that host APBA3 supports the metastatic efficiency of tumor cells.

Host APBA3 Promotes Early Colonization of Cancer Cells in the Lung. To characterize the roles of host APBA3 in metastatic cascades, we first evaluated metastatic tumor growth by measuring the diameter of lung metastatic foci. The size distribution of metastatic B16F10 cell foci was not significantly different between WT and *Apba3*$^{-/-}$ mice (Fig. 2 *A* and *B*), suggesting that host APBA3 deficiency does not affect metastatic nodule growth.

Emerging studies using single-cell imaging techniques have identified tumor cell-autonomous and nonautonomous regulators of early colonization (23, 24). Thus, we next evaluated the early steps in lung colonization by i.v. injecting fluorescently labeled tumor cells. The number of tumor cells in the lungs was similar in both types of mice at 1 h after inoculation, suggesting that the circulation of tumor cells is not perturbed in *Apba3*$^{-/-}$ mice (Fig. 2 *C* and *D* and Fig. S1*A*). At 24 h postinoculation, B16F10 cells in the lungs decreased; interestingly, fewer cells remained in the lungs of *Apba3*$^{-/-}$ mice than those of WT mice (Fig. 2 *C* and *D* and Fig. S1*A*).

We then evaluated the precise localization of tumor cells in the lung by whole-mount staining with anti-CD31 antibodies. As previously reported (5, 25), all tumor cells were surrounded by CD31-positive lung capillaries in both genotypes at 1 h (Fig. 2 *E* and *F* and Fig. S1*B*). However, half of the tumor cells invaded the interstitium in the lungs of WT mice at 24 h, whereas only 25% of tumor cells did so in *Apba3*$^{-/-}$ mice (Fig. 2 *E* and *F* and Fig. S1*B*). Consistent with the data obtained with B16F10 cells, injection with fluorescently labeled LLC cells and 4T1 cells demonstrated that APBA3 deficiency in host cells caused reduced lung colonization and extravasation (Fig. S1 *C*–*F*). Thus, host APBA3 promotes extravasation and colonization of cancer cells.

APBA3 Supports Metastasis Formation via Induction of E-Selectin Expression in the Lung. Tumor adhesion to endothelial cells is crucial to the survival and extravasation of tumor cells. Thus, we analyzed the expression of endothelial adhesion molecules that correlates with lung metastasis. Among these, only *Sele* (E-selectin)

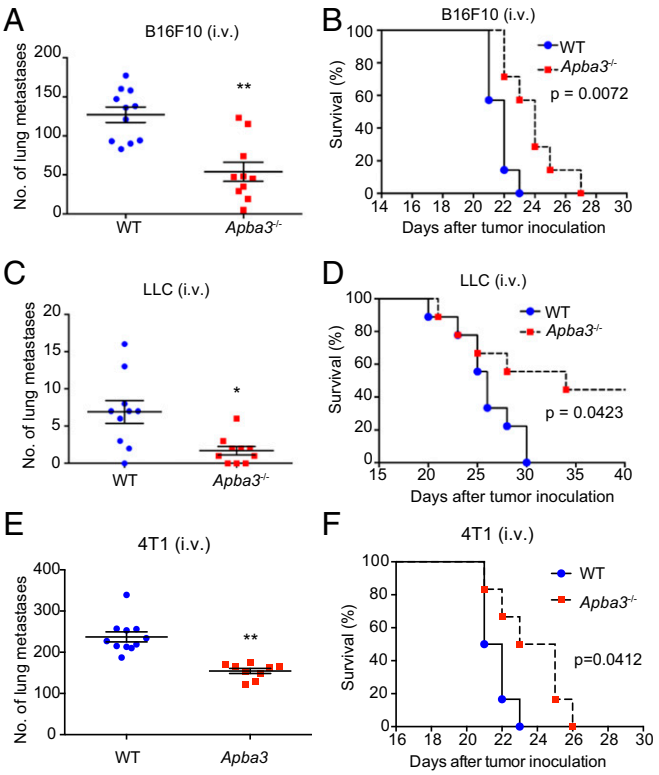

Fig. 1. Host APBA3 deficiency affects metastasis. (*A*) Lung metastatic burden of i.v.-injected B16F10 cells 14 d after inoculation in WT (n = 11) or *Apba3*$^{-/-}$ mice (n = 10). (*B*) Survival of WT or *Apba3*$^{-/-}$ mice after i.v. injection with B16F10 cells. n = 7 per group. (*C*) Lung metastatic burden of i.v.-injected LLC cells at 14 d after inoculation in WT or *Apba3*$^{-/-}$ mice. n = 10 per group. (*D*) Survival of WT or *Apba3*$^{-/-}$ mice after i.v. injection with LLC cells. n = 9 per group. (*E*) Lung metastatic burden of i.v.-injected 4T1 cells at 14 d after inoculation in WT (n = 11) or *Apba3*$^{-/-}$ mice (n = 9). (*F*) Survival of WT or *Apba3*$^{-/-}$ mice after i.v. injection with 4T1 cells. n = 6 per group. Data represent mean ± SEM. $*P < 0.05$, $**P < 0.01$, as determined by the Mann–Whitney *U* test.

mRNA expression was significantly and ectopically induced after tumor inoculation (Fig. S2), which correlated with observations in the liver by other groups (26, 27). Notably, *Sele* mRNA levels at 4 h were significantly lower in the lungs of *Apba3*$^{-/-}$ than WT mice (Fig. S2*A*). Consistent with this, immunostaining revealed that tumor-induced expression of E-selectin was observed 6 h after tumor inoculation, although no E-selectin signal was detected in untreated WT mouse lungs (Fig. 3 *A* and *B*). Importantly, fewer E-selectin–positive cells were observed in the lungs of tumor-inoculated *Apba3*$^{-/-}$ mice (Fig. 3*B*). Furthermore, E-selectin–positive cells were elongated and expressed the endothelial marker CD31 (Fig. 3*C*), suggesting that host APBA3 stimulates endothelial cells to express E-selectin in the lung.

To examine whether the induced E-selectin promoted metastasis, neutralizing antibodies were administered to mice before tumor inoculation. E-selectin–neutralizing antibodies decreased metastatic foci on the lungs of WT mice to *Apba3*$^{-/-}$ mouse levels (Fig. 3 *D* and *E*) but did not affect metastatic formation in *Apba3*$^{-/-}$ mice (Fig. 3 *D* and *E*). Thus, APBA3 expression in the target organ promotes metastasis via tumor-induced expression of E-selectin in lung endothelial cells.

Myeloid Cell-Derived VEGFA Induces E-Selectin Expression in the Lungs. Several soluble factors induce E-selectin expression in endothelial cells (28), including VEGFA, encoded by a target gene of HIF (29), whereby cancer cells home in on the lungs

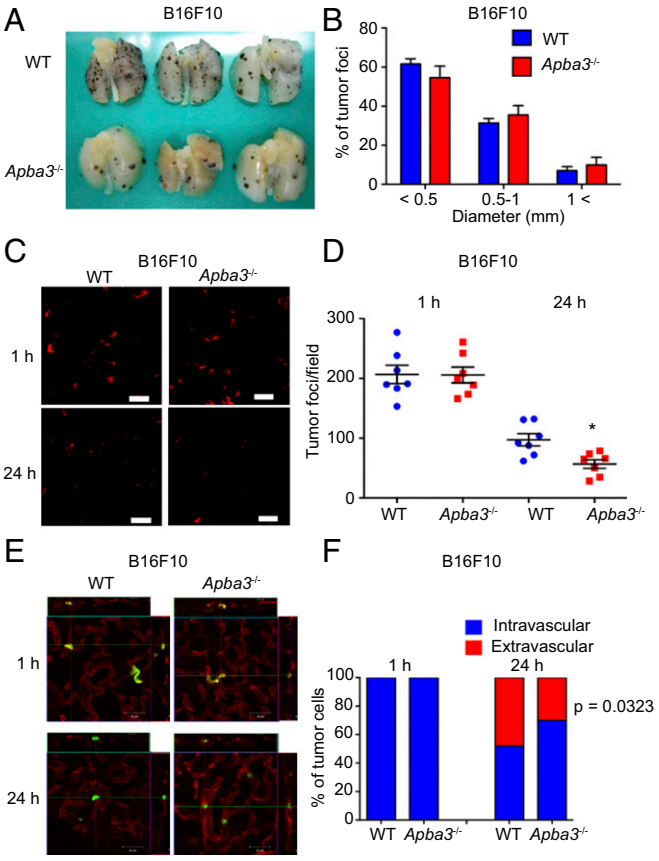

Fig. 2. Host APBA3 deficiency decreases metastatic colonization and extravasation. (*A* and *B*) Macroscopic analysis of metastatic growth of B16F10 cells in the lungs of WT and *Apba3*$^{-/-}$ mice. (*A*) Representative photo of metastatic lungs from WT and *Apba3*$^{-/-}$ mice. (*B*) Metastatic growth was quantified and categorized by measuring the diameter of foci. $n = 3$ (18 to 74 foci) per group. (*C* and *D*) Colonization of B16F10 cells in the lungs of WT or *Apba3*$^{-/-}$ mice 1 or 24 h after i.v. inoculation. (*C*) Representative photos of B16F10 cell colonies (red) in the lungs. (Scale bars, 100 μm.) (*D*) The number of tumor foci was counted. $n = 7$ per group. $^{*}P < 0.05$, as determined by the Mann–Whitney *U* test. (*E* and *F*) Confocal microscopic analysis of B16F10 cells (green) and endothelial cells (CD31; red) in the lungs of WT or *Apba3*$^{-/-}$ mice. (*E*) Representative photos. (Scale bars, 20 μm.) (*F*) The ratio of intravascular and extravascular B16F10 cells was analyzed. $n = 45$ to 68 cells. $P < 0.05$, as determined by Fisher's exact test. Data are represented as mean ± SEM.

(30). To test whether VEGFA also plays a role in E-selectin expression in our experimental metastasis model, we administered a VEGFA-neutralizing antibody before tumor cell injection. This was verified by our finding that, compared with control IgG, the neutralizing antibodies markedly suppressed tumor cell-induced E-selectin expression in the lungs (Fig. 4*A*).

Next, we investigated the cells that act as a source of VEGFA in metastatic lungs. We first examined whether tumor cell-derived VEGFA induces E-selectin in metastatic lungs. However, VEGFA suppression by shRNA in B16F10 cells did not affect E-selectin induction (Fig. S3). Then, we examined VEGFA-expressing cells in metastatic lungs. Immunostaining experiments revealed that some cells express VEGFA in lungs by costaining VEGFA with cellular markers for cancer cells and leukocytes. Interestingly, VEGFA-expressing cells were all CD45-positive leukocytes. Among VEGFA-expressing cells, ∼80% were CD68-positive, macrophage-lineage cells and ∼60% were CD11c-positive myeloid cells, including dendritic cells and some types of macrophages; however, the cells were negative for T-cell (CD4 and CD8) and B-cell (B220) markers (Fig. 4 *B* and *C*). Thus, macrophage-lineage cells were the main source of VEGFA in metastatic lungs. Indeed, we observed clusters of B16F10 cells, macrophages, and endothelial E-selectin in metastatic lungs (Fig. 4*D*). Because APBA3 depletion selectively affects macrophages (20), we used the LysM-cre conditional knockout mouse model. Mice specifically APBA3-deficient in myeloid cells including macrophages (LysM-cre; *Apba3*$^{fl/fl}$) exhibited defects in tumor-induced E-selectin expression and suppressed tumor metastasis to the lungs in comparison with control animals (Fig. 4 *E* and *F*), suggesting that macrophage-lineage cells suppress metastasis in *Apba3*$^{-/-}$ mice.

Because LysM-cre mice express cre recombinase in neutrophils (NEs) as well as in monocytes/macrophages, we further confirmed the effect of APBA3 in monocytes/macrophages using liposome-encapsulated clodronate (L-clodronate) (31). Upon depletion of monocytes, metastasis was suppressed significantly (Fig. S4), confirming that monocytes/macrophages promote metastasis.

Loss of APBA3 Decreases IMs at Metastatic Sites. Among macrophage-lineage cells, IMs strongly expressed VEGFA and thereby promoted endothelial permeability, tumor extravasation, and metastasis (14). Thus, we further focused on the function of APBA3 in IMs. We evaluated the number of IMs in WT and *Apba3*$^{-/-}$ mice with or without tumor inoculation; this number was similar in the BM and peripheral blood of *Apba3*$^{-/-}$ and WT mice, although

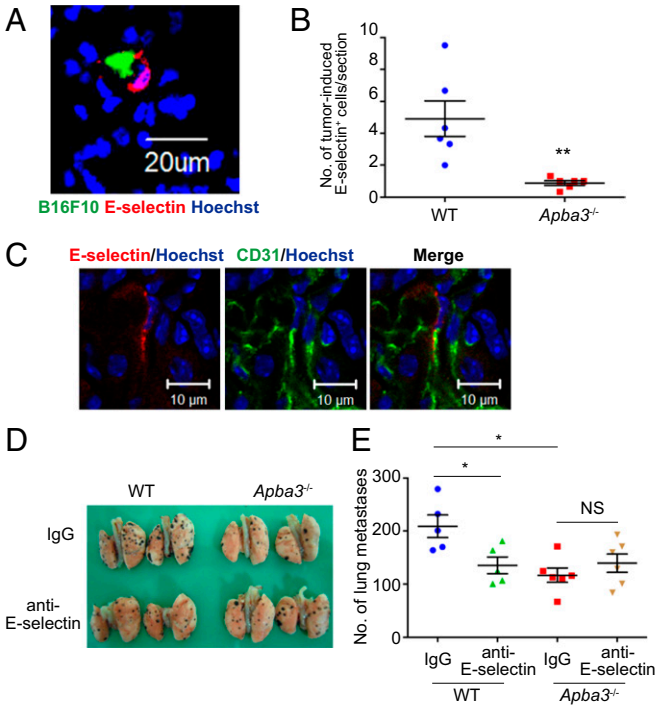

Fig. 3. Host APBA3 deficiency decreases tumor-induced E-selectin expression in endothelial cells. (*A* and *B*) Immunostaining of E-selectin in the lungs at 6 h after i.v. injection with B16F10 cells (green). (*A*) Representative photo of E-selectin (red) and B16F10 cells (green) in the lungs of WT mice. (Scale bar, 20 μm.) (*B*) Tumor-induced E-selectin–positive cells were counted. $n = 6$. (*C*) Immunostaining of E-selectin (red) and CD31 (green) in the lungs of WT mice 6 h after i.v. injection with B16F10 cells. (Scale bars, 10 μm.) (*D* and *E*) Analysis of lung metastatic burden at 14 d after i.v. injection with E-selectin–neutralizing antibody or rat IgG followed by B16F10 cell inoculation in WT or *Apba3*$^{-/-}$ mice. (*D*) Representative photos of metastatic lungs. (*E*) The number of metastatic foci on the lungs was counted. $n = 5$ or 6 per group. Data are represented as mean ± SEM. $^{*}P < 0.05$, $^{**}P < 0.01$, as determined by the Mann–Whitney *U* test. NS, not significant.

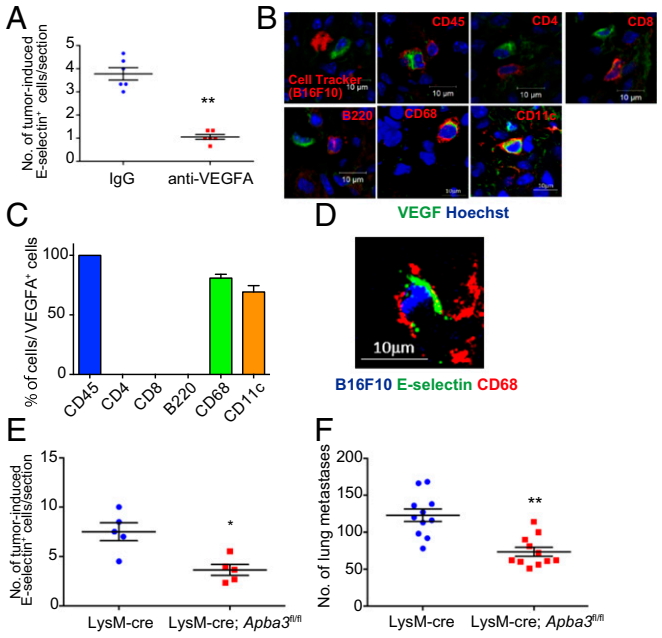

Fig. 4. VEGFA inhibition and APBA3 deficiency in myeloid cells hamper E-selectin induction. (*A*) Immunostaining analysis of E-selectin in the lungs at 6 h after i.v. injection with VEGFA-neutralizing antibody or goat IgG followed by B16F10 cell inoculation in WT mice. Tumor-induced E-selectin–positive cells were counted. $n = 5$ per group. (*B* and *C*) Immunostaining analysis of VEGFA and cellular markers in the lungs of WT mice 6 h after i.v. injection with B16F10 cells. (*B*) Representative photos of VEGFA (green) and cellular markers (red) in the lungs. (Scale bars, 10 μm.) (*C*) The ratios of cellular marker-positive cells and VEGFA-positive cells were analyzed. $n = 3$ (21 to 130 cells) per group. (*D*) Immunostaining analysis of CD68 (red) and E-selectin (green) expression in the lungs of WT mice 6 h after i.v. injection with fluorescein-labeled B16F10 cells (blue). (Scale bar, 10 μm.) (*E*) Quantified analysis of E-selectin–positive cells in the lungs of LysM-cre (control) or LysM-cre; *Apba3*$^{fl/fl}$ mice 6 h after i.v. injection with B16F10 cells. $n = 5$. (*F*) Lung metastatic burden in LysM-cre (control) or LysM-cre; *Apba3*$^{fl/fl}$ mice 14 d after i.v. injection with B16F10 cells. $n = 11$ per group. Data represent mean ± SEM. $^*P < 0.05$, $^{**}P < 0.01$, as determined by the Mann–Whitney *U* test.

IMs were fewer in the spleen (Fig. 5*A* and Fig. S5). When mice were inoculated with B16F10 cells, the number of IMs increased in the peripheral blood of WT mice but not in *Apba3*$^{-/-}$ mice (Fig. 5*B*). Interestingly, fewer IMs were observed in the lungs of *Apba3*$^{-/-}$ mice, even without tumor inoculation (Fig. 5*C*). Although the IM number in the lungs increased upon tumor inoculation, there were fewer IMs in *Apba3*$^{-/-}$ than in WT mice. In contrast, NE and resident monocyte numbers were similar in the lungs of WT and *Apba3*$^{-/-}$ mice, with or without tumor inoculation (Fig. 5 *D* and *E*). Mice with conditional APBA3 knockout in myeloid cells also showed decreased IMs in the lungs after tumor inoculation (Fig. 5*F*), implying that recruitment of IMs to metastatic sites in *Apba3*$^{-/-}$ is intrinsically defective.

APBA3 in IMs Is Required for Glycolysis-Dependent Chemotaxis, VEGFA Expression, and Metastasis Formation. IMs express chemokine receptor CCR2; the CCR2 ligand, CCL2, released by inflamed tissues, recruits IMs from the BM to the peripheral blood and inflamed tissues (13). CCL2 levels increased after tumor inoculation, but there was no difference in CCL2 levels in the lungs or peripheral blood between WT and *Apba3*$^{-/-}$ mice (Fig. S6 *A* and *B*). CCR2 expression on the IM cell surface was similar in WT and *Apba3*$^{-/-}$ mice (Fig. S6*C*); thus, loss of APBA3 does not affect CCL2/CCR2 expression levels.

Subsequently, the in vivo chemotaxis capacity of control and *Apba3*$^{-/-}$ IMs was tested by i.p. injection with recombinant CCL2. IMs accumulated in the peritoneal cavity at 6 h after CCL2 injection, which was significantly attenuated in mice with conditional APBA3 knockout in myeloid cells (Fig. 6*A*). Therefore, *Apba3*$^{-/-}$ IMs are defective in chemotaxis toward CCL2 in vivo.

Previously, we had reported that *Apba3*$^{-/-}$ BM-derived macrophages are defective in chemotaxis due to reduced glycolytic production of ATP that is caused by low HIF activity (20). We found that the glycolysis inhibitor 2-deoxyglucose (2-DG) abolished in vivo chemotaxis of IMs toward CCL2 (Fig. 6*B*). To investigate the impact of glycolytic regulation on APBA3-driven metastatic processes, we treated mice with 2-DG 10 h before tumor inoculation. Pretreatment with 2-DG significantly suppressed IM recruitment to the metastatic lungs of WT and *Apba3*$^{-/-}$ mice, and the number of IMs in 2-DG–pretreated metastatic lungs was comparable to that in nonmetastatic lungs (Figs. 5*C* and 6*C*). 2-DG pretreatment decreased the number of VEGFA-positive cells and E-selectin induction in metastatic lungs, as well as metastasis in WT mice, to the levels in *Apba3*$^{-/-}$ mice (Fig. 6 *D*–*F*). Treating B16F10 cells with 2-DG in vitro followed by i.v. injection did not affect metastatic formation (Fig. S7). Thus, host APBA3 regulates IM recruitment via glycolytic regulation to support metastasis.

We next sought to analyze APBA3-mediated glycolytic regulation in IMs. *Apba3*$^{-/-}$ IM ATP levels were decreased by ca. 40%, compared with WT IMs (Fig. 6*G*, vehicle). The ATP levels in WT and *Apba3*$^{-/-}$ IMs decreased, and the differences between them became negligible, in the presence of 2-DG (Fig. 6*G*, 2-DG). HIF-1α–deficient (*Hif1a*$^{-/-}$) IMs also exhibited defective glycolysis-dependent ATP production, as reported for macrophages (17), comparable to that observed in *Apba3*$^{-/-}$ IMs (Fig. 6*G*).

HIF-1 promotes expression of glycolysis-related genes, whereas APBA3 promotes glycolysis by activating HIF-1 in macrophages (19–21). We evaluated the expression of glycolysis-related genes, including enzymes mediating all glycolysis steps, and two HIF-1–targeted glucose transporters in WT, *Apba3*$^{-/-}$, and *Hif1a*$^{-/-}$ IMs by real-time RT-PCR. Expression levels of most tested genes in *Apba3*$^{-/-}$ IMs decreased to ∼50 to 80% of those in WT IMs, and were comparable to those in *Hif1a*$^{-/-}$ IMs (Fig. 6*H*). Thus, APBA3 promotes glycolysis-related gene expression and ATP production, facilitating IM chemotaxis.

Moreover, expression levels of *Vegfa* mRNA, one of the major targets of HIF, also decreased in *Apba3*$^{-/-}$ IMs, to those in *Hif1a*$^{-/-}$ IMs (Fig. 6*I*). This may be another reason for the suppression of metastasis in *Apba3*$^{-/-}$ mice. To investigate this, WT IMs were adoptively transferred to WT and *Apba3*$^{-/-}$ mice with tumor inoculation; this did not affect metastasis in WT mice but increased metastasis in *Apba3*$^{-/-}$ mice (Fig. 6*J*). Thus, regulation of IM function by APBA3 promotes metastasis.

Host APBA3 Controls the Metastatic Microenvironment in the Spontaneous Metastasis Model. Although we used an experimental metastasis model, this model may differ from spontaneous metastasis because it involves a large number of tumor cells arriving in the lungs concurrently. Furthermore, recently, primary tumor-derived factors, such as exosomes, cytokines, and chemokines, including CCL2, have been suggested to modulate secondary sites, facilitating the creation of a favorable niche for disseminated and circulating tumor cells (32–34). B16F10 cells, which were established on the basis of their lung-colonizing ability after serial i.v. injections (35), showed high metastatic capabilities from the tail vein, but we could not observe any metastatic colonies on the lungs 3 to 4 wk after s.c. injection of B16F10 cells into the dorsal flank as previously reported by others (36). We therefore examined spontaneous lung metastasis models with LLC cells inoculated s.c. and 4T1 cells inoculated into the mammary fat pad. LLC and 4T1 cells grew at the inoculated sites

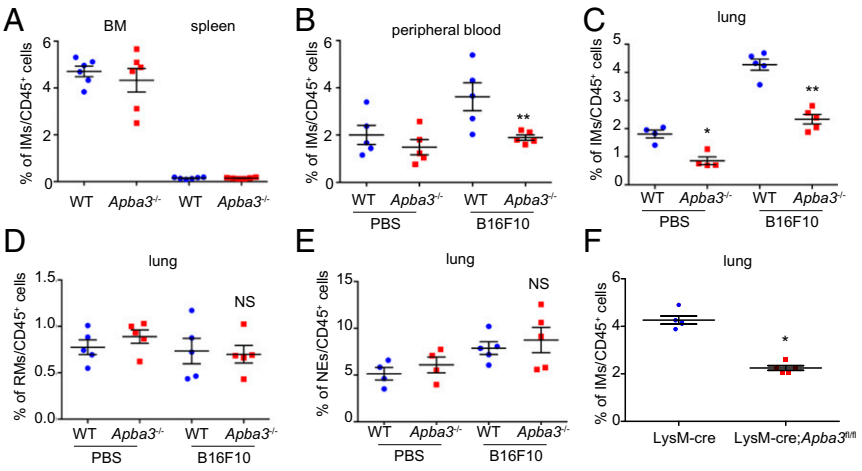

Fig. 5. APBA3 deficiency attenuates chemotaxis of inflammatory monocytes to metastatic sites. (*A*) Flow cytometric analysis of IMs in the bone marrow and spleen of WT or *Apba3*$^{-/-}$ mice. $n = 6$ per group. (*B* and *C*) Flow cytometric analysis of IMs in the peripheral blood (*B*) and lungs (*C*) of WT or *Apba3*$^{-/-}$ mice 4 h after i.v. injection with B16F10 cells or PBS. $n = 4$ or 5 per group. (*D* and *E*) Flow cytometric analysis of resident monocytes (*D*) and neutrophils (*E*) in the lungs at 4 h after i.v. injection with B16F10 cells or PBS in WT or *Apba3*$^{-/-}$ mice. $n = 4$ or 5 per group. (*F*) Flow cytometric analysis of IMs in the lungs at 4 h after i.v. injection with B16F10 cells in WT or LysM-cre; *Apba3*$^{fl/fl}$ mice. $n = 5$ per group. Data represent mean ± SEM. $^{*}P < 0.05$, $^{**}P < 0.01$, as determined by the Mann–Whitney *U* test.

comparably in WT and *Apba3*$^{-/-}$ mice (Fig. 7 *A* and *B*). However, *Apba3*$^{-/-}$ mice showed decreased spontaneous lung metastasis with LLC and 4T1 cells (Fig. 7 *C* and *D*), similar to the results obtained with the experimental metastasis model (Fig. 1 *C* and *E*). Next, we analyzed IM recruitment and VEGFA and E-selectin expression in the lungs before macroscopic formation of metastatic foci. At 14 d after s.c. inoculation with LLC cells and at 7 d after mammary fat pad inoculation with 4T1 cells, IMs accumulated markedly, and VEGFA and E-selectin expression was induced in the lungs (Fig. 7 *E*–*J*); however, APBA3 deficiency decreased both phenomena (Fig. 7 *E*–*J*). Therefore, host APBA3 appears to modulate the metastatic microenvironment in the target organ of LLC and 4T1 spontaneous metastasis models.

Discussion

Monocyte/macrophage-lineage cells are abundant in the tumor microenvironment and essential in metastasis (37). Tumor cells exploit the marked sensitivity and naivety of these cells to environmental stimuli by unknown molecular mechanisms. Here we show that APBA3 deficiency in the metastatic microenvironment, particularly in IMs, suppresses metastasis. APBA3 in IMs activates glycolysis-dependent ATP production and thereby promotes chemotaxis from the BM to the peripheral blood and metastatic tissues. In addition, APBA3 promotes VEGFA expression in IMs. At metastatic sites, VEGFA-induced E-selectin expression by endothelial cells supports extravasation of cancer cells, resulting in metastasis (Fig. 8). Thus, our study using *Apba3*$^{-/-}$ mice has partly elucidated the complicated network among tumor cells, immune cells, and endothelial cells in the establishment of metastasis.

In this study, we focused on E-selectin induction by VEGFA in IMs. In addition to E-selectin induction, VEGFA can also promote vascular leakiness. Indeed, *Apba3*$^{-/-}$ mice showed reduced vascular leakiness in metastatic lungs than did WT mice (Fig. S8 *A* and *B*). Thus, VEGFA-mediated vascular leakiness might also contribute to host APBA3-mediated metastasis. However, E-selectin–neutralizing antibodies decreased B16F10 metastasis in WT lungs to the levels of *Apba3*$^{-/-}$ lungs (Fig. 3 *D* and *E*) without affecting vascular leakiness (Fig. S8 *C* and *D*). Thus, E-selectin is indispensable for host APBA3-mediated metastasis.

HIF-1 is a master regulator of glycolysis, and depletion of HIF-1α decreases ATP production in macrophages, which depend on glycolysis for their ATP production, even during normoxia (17). *Apba3*$^{-/-}$ IMs showed decreased expression of glycolysis-related genes and glycolysis-dependent ATP production, comparable to those of *Hif1a*$^{-/-}$ IMs. Thus, APBA3 seems to be a major regulator of HIF-1 via FIH-1 inhibition in IMs during normoxia. Oxygen-dependent FIH-1 activity can be suppressed under more severely hypoxic conditions than prolyl hydroxylase domain (PHD) (38). APBA3-mediated HIF activation also becomes negligible under severely hypoxic conditions, when FIH-1 function ceases (39). Because IMs are present in blood vessels, where oxygen supply is sufficient, the pathophysiological roles of APBA3 can be studied in IMs.

CCL2 is produced by tumor and stromal cells, such as mesenchymal stem cells and fibroblasts (15, 40, 41). CCL2 levels in the lungs and peripheral blood increased significantly after tumor inoculation (Fig. S6 *A* and *B*), followed by accumulation of IMs and NEs, but not RMs, in the lungs (Fig. 5 *C*–*E*). CCL2 recruits both metastasis-promoting IMs and -suppressive NEs (4, 14), although only recruitment of IMs was affected in tumor-inoculated *Apba3*$^{-/-}$ mice (Fig. 5*C*), perhaps because glycolytic regulation by APBA3 is specific for macrophages but not for NEs (20). Thus, APBA3 is a possible target for metastasis suppression by targeting monocyte/macrophage-specific machineries. CCL2 functions not only as a chemoattractant, as it has also been reported to induce VEGFA expression by regulating VEGFA mRNA transcription and stability (42, 43). Thus, CCL2 produced by tumor and stromal cells might contribute to VEGFA expression in IMs. Interestingly, CCR2-deficient mice show decreased IM recruitment and *Sele* mRNA expression in the lungs after tumor inoculation (44), which is similar to our *Apba3*$^{-/-}$ mouse results. Interestingly, few IMs were observed in the lungs of C57BL/6-background *Apba3*$^{-/-}$ mice, but not in those of BALB/cA-background *Apba3*$^{-/-}$ mice (Figs. 5*C* and Figs. 7 *E* and *F*). However, even in C57BL/6-background mice, 2-DG pretreatment completely suppressed APBA3-mediated IM recruitment, VEGFA and E-selectin induction, and metastasis in the lungs (Fig. 6 *C*–*F*). Thus, IMs recruited to the lungs (rather than IMs preexisting in the lungs) likely play a main role in preparing the metastatic niche.

In this study, we focused on the metastatic niche formation by IMs and found that APBA3 controls IM function in metastatic niche formation. The premetastatic niche is primed and organized in distant organs by primary tumors to support the colonization of CTCs (45). Secreted factors such as chemokines, cytokines, and exosomes from primary tumors mainly mobilize bone marrow-derived cells (BMDCs) to facilitate the invasion and

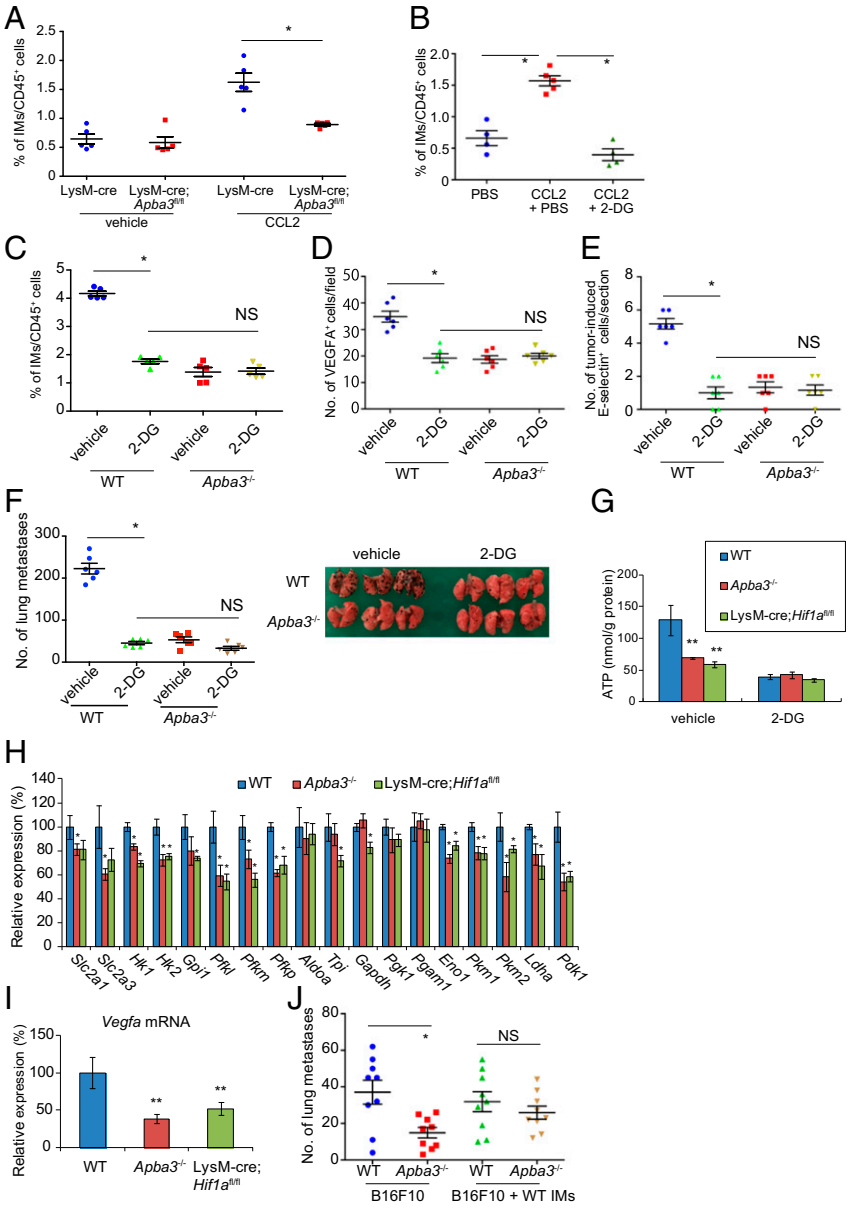

Fig. 6. APBA3 deficiency in IMs attenuates glycolysis-dependent chemotaxis, VEGF expression, and metastasis. (*A*) Flow cytometric analysis of peritoneal IMs at 6 h after i.p. injection with recombinant CCL2 in LysM-cre or LysM-cre; *Apba3*$^{fl/fl}$ mice. $n = 5$ per group. (*B*) Flow cytometric analysis of peritoneal IMs at 6 h after i.p. injection with recombinant CCL2, following administration with a glycolytic inhibitor, 2-deoxyglucose, in WT mice. $n = 4$ or 5 per group. (*C*) Flow cytometric analysis of IMs in the lungs at 4 h after i.v. injection with B16F10 cells in WT or *Apba3*$^{-/-}$ mice treated with or without 2-DG. $n = 5$ per group. (*D*) Quantitative analysis of VEGFA-positive cells in the lungs of vehicle- or 2-DG–administered WT or *Apba3*$^{-/-}$ mice 6 h after i.v. injection with B16F10 cells. $n = 6$ per group. (*E*) Quantitative analysis of E-selectin–positive cells in the lungs of vehicle- or 2-DG–administered WT or *Apba3*$^{-/-}$ mice 6 h after i.v. injection with B16F10 cells. $n = 6$ per group. (*F*) The number of metastatic foci and the representative photos of lungs in vehicle- or 2-DG–administered WT or *Apba3*$^{-/-}$ mice 14 d after i.v. injection with B16F10 cells. $n = 6$ per group. (*G*) ATP levels in WT, *Apba3*$^{-/-}$, and LysM-cre; *Hif1a*$^{fl/fl}$ IMs with or without 2-DG. $n = 3$ per group. (*H*) mRNA levels of glycolysis-related genes in WT, *Apba3*$^{-/-}$, and LysM-cre; *Hif1a*$^{fl/fl}$ IMs. $n = 3$ per group. (*I*) *Vegfa* mRNA levels in WT, *Apba3*$^{-/-}$, and LysM-cre; *Hif1a*$^{fl/fl}$ IMs. $n = 3$ per group. (*J*) Lung metastatic burden in WT or *Apba3*$^{-/-}$ mice 14 d after tail vein injection with B16F10 cells with or without WT IMs. $n = 9$ per group. (*A–F* and *J*) Error bars indicate the SEM. (*G–I*) Error bars indicate the SD. $*P < 0.05$, $**P < 0.01$, as determined by the Mann–Whitney *U* test (*A–F* and *J*) or Student's *t* test (*G–I*).

survival of CTCs at the target organs (32–34). These BMDCs consist of diverse cellular components, including CCL2/CCR2-recruited IMs (41). Interestingly, even in the spontaneous metastasis models of LLC and 4T1 cells, APBA3 deficiency suppressed tumor inoculation-induced increase of IMs, VEGFA-positive cells, and E-selectin expression in the lungs when no metastasis was observed in the lungs (Fig. 7 *E–J*). Thus, APBA3 might also control premetastatic niche formation via IMs.

Monocytes located around vasculature are involved in vascular functions under physiological and pathological conditions (46, 47). In our study, IMs expressed VEGFA, a key inducer of tumor-associated E-selectin expression in endothelial cells in the lungs during metastasis. However, IMs also express endothelial modulators, such as TNF-α, inducible NOS, and reactive oxygen species, in pathogen-based infectious models (48, 49). It remains possible that intermediates other than VEGFA from IMs also contribute to E-selectin induction and vascular modulation.

Intravenous injection of liposome–clodronate, which depletes circulating monocytes/macrophages but not extravascular cells because it cannot penetrate through the vascular barrier (50),

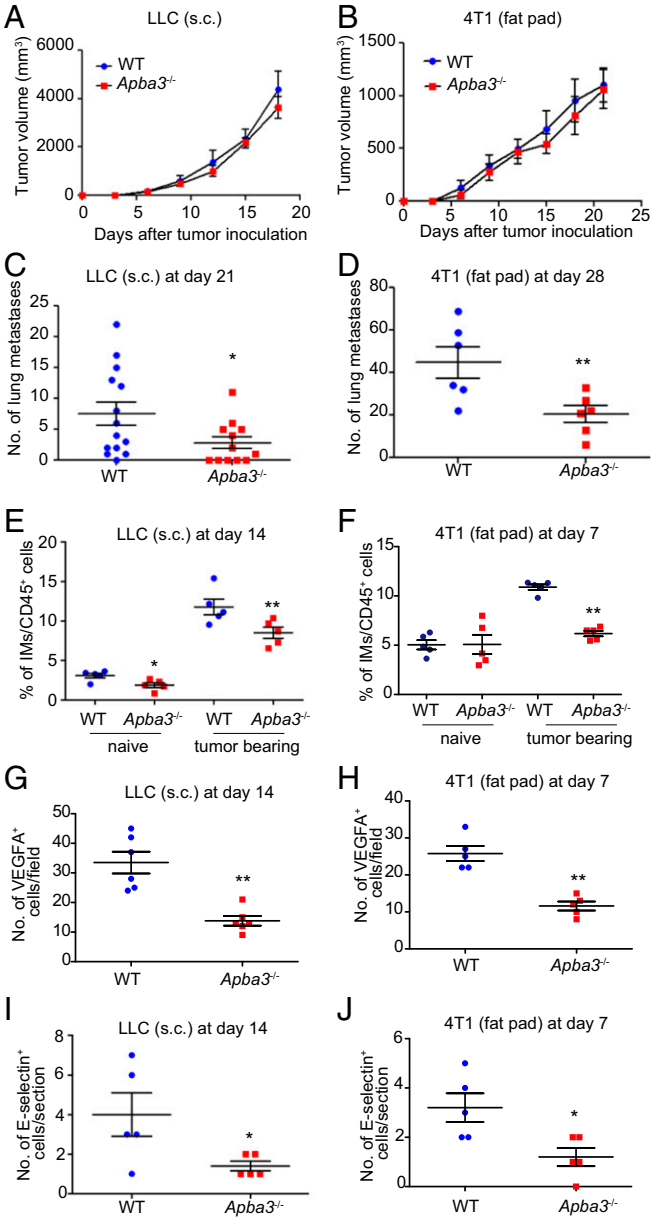

Fig. 7. Host APBA3 governs a metastatic microenvironment in spontaneous lung metastasis. (*A*) Subcutaneous tumor growth of Lewis lung carcinoma cells in WT ($n = 6$) or *Apba3*$^{-/-}$ mice ($n = 7$). (*B*) Tumor growth of 4T1 cells in the fat pad of WT or *Apba3*$^{-/-}$ mice. $n = 6$ per group. (*C*) Spontaneous lung metastatic burden of LLC cells 21 d after inoculation in WT ($n = 14$) or *Apba3*$^{-/-}$ mice ($n = 12$). (*D*) Spontaneous lung metastatic burden of 4T1 cells 28 d after inoculation in WT or *Apba3*$^{-/-}$ mice. $n = 6$ per group. (*E*) Flow cytometric analysis of IMs in the lungs at 14 d after s.c. injection with LLC cells in WT or *Apba3*$^{-/-}$ mice. $n = 5$ per group. (*F*) Flow cytometric analysis of IMs in the lungs at 7 d after fat pad injection with 4T1 cells in WT or *Apba3*$^{-/-}$ mice. $n = 5$ per group. (*G*) Immunostaining analysis of VEGFA in the lungs of LLC tumor-bearing WT or *Apba3*$^{-/-}$ mice at 14 d after tumor inoculation. $n = 6$ per group. (*H*) Immunostaining analysis of VEGFA in the lungs of 4T1 tumor-bearing WT or *Apba3*$^{-/-}$ mice at 7 d after tumor inoculation. $n = 5$ per group. (*I*) Immunostaining analysis of E-selectin in the lungs of LLC tumor-bearing WT or *Apba3*$^{-/-}$ mice at 14 d after tumor inoculation. $n = 5$ per group. (*J*) Immunostaining analysis of E-selectin in the lungs of 4T1 tumor-bearing WT or *Apba3*$^{-/-}$ mice at 7 d after tumor inoculation. $n = 5$ per group. Data represent mean ± SEM. $^{*}P < 0.05$, $^{**}P < 0.01$, as determined by the Mann–Whitney *U* test.

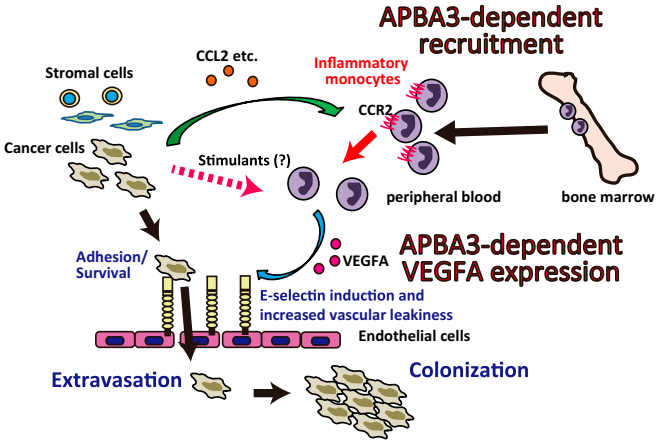

Fig. 8. Schematic illustration of APBA3-mediated metastasis. Cancer and/or stromal cells at the metastatic sites secrete chemokines (e.g., CCL2). Inflammatory cells, including inflammatory monocytes, migrate toward chemokines. APBA3 in IMs promotes glycolysis-dependent chemotaxis to the metastatic sites. APBA3 also promotes VEGFA transcription in IMs. IMs at metastatic sites secrete VEGFA, which induces E-selectin expression in endothelial cells and vascular permeability. Cancer cells take advantage of E-selectin in endothelial cells, facilitating efficient extravasation and metastasis.

effectively reduced APBA3-mediated metastasis (Fig. S4). Thus, APBA3 seems to be necessary for intravascular monocytes/macrophages to form the metastatic niche in the lungs. However, it remains unclear whether APBA3-mediated metastatic niche formation is induced by IMs in the blood or those migrating to the lung tissues from the blood. Recently, both intravascular and extravascular monocytes/macrophages have been reported to associate with extravasation of tumor cells in the lungs (14, 51). Thus, APBA3-mediated metastatic niche formation might also be regulated by both intravascular and extravascular monocytes/macrophages.

E-selectin is an endothelial cell-expressed cell-adhesion molecule that allows recognition of these cells by inflammatory cells and metastatic tumor cells (28, 52); it also functions as a niche component of hematopoietic stem cells, promoting dormancy and chemoresistance (53). Binding between VCAM1 on breast cancer cells and α4-integrin on macrophages transmits survival signals to cancer cells in metastatic lungs (3). Thus, expression of E-selectin on lung endothelial cells may provide attached tumor cells a means not only for extravasation but also to transmit survival signals.

In conclusion, we show that stromal APBA3 depletion hampers metastasis by suppressing chemotaxis and VEGFA expression in IMs. In association with the myeloid compartments, endothelial cells help form the metastatic niche, representing a potentially novel means of preventing metastatic diseases. Thus, our findings help dissect one aspect of the complicated cellular and molecular cascades involved in metastatic initiation via the *Apba3* gene. These and previous findings together indicate that APBA3 may be a therapeutic target for the control of both tumor and stromal cells.

Materials and Methods

Animals. Animals were maintained under specific pathogen-free conditions and experiments were performed according to institutional animal ethical and safety guidelines for gene manipulation experiments (Institute of Medical Science, The University of Tokyo). APBA3-deficient (*Apba3*$^{-/-}$) and APBA3-floxed (*Apba3*$^{fl/fl}$) mice (20) [RIKEN Center for Developmental Biology (CDB) accession no. CDB0589K] were backcrossed into the C57BL/6J (CLEA Japan) background for at least 12 generations. *Apba3*$^{-/-}$ mice were also backcrossed into the BALB/c (CLEA Japan) background for at least 8 generations. LysM-cre (54) and *Hif1a*$^{-/-}$ (C57B/6J background) mice were purchased from The Jackson Laboratory (stock nos. 004781 and 007561, respectively).

Cell Culture. B16F10 melanoma and LLC cells were obtained from the Cell Resource Center for Biomedical Research, Institute of Development, Aging and Cancer, Tohoku University. 4T1 breast cancer cells were obtained from the American Type Culture Collection. B16F10 and LLC cells were cultured in DMEM (low-glucose) supplemented with 10% FBS.

Tumor Transplantation. Six- to 10-wk-old female mice were used for growth and metastasis assays. To evaluate spontaneous metastasis, 4×10^5 LLC cells in 0.2 mL of PBS were injected into the left flank of the mice, which were killed at day 21. Lung metastatic foci were counted under a stereoscopic microscope. For the lung metastasis assay, 4×10^5 B16F10 or LLC cells in 0.2 mL of PBS were injected via the lateral tail vein, and the mice were killed 14 d later. To evaluate the size distribution of the metastatic foci, the lungs were photographed alongside a ruler and categorized by size into three groups. To inhibit glycolytic activity in host cells, 0.5 g/kg body weight (b.w.) of 2-DG was administered intraperitoneally 10 h before tumor inoculation. For tumor-specific glycolysis inhibition, B16F10 cells were incubated with 200 μg/mL 2-DG for 1 h, followed by i.v. injection.

Lung Colonization and Extravasation Assay. Lung colonization assays (55) and extravasation assays were performed as previously described (5). Fluorescently labeled cells in the lungs were counted by confocal microscopy (Carl Zeiss).

RNA Extraction and RT-qPCR. Lung tissues were snap-frozen in liquid N_2 and crushed to powder in a mortar. Total RNA isolation from powdered tissues or cells, reverse transcription, and RT-PCR were performed with specific primers (Table S1) as previously described (20, 56). mRNA expression levels were normalized to that of *Actb* (β-actin) mRNA.

Immunohistochemistry. Immunohistochemistry was performed as previously described (22) using the antibodies listed in Table S2. Fluorescent images were taken by confocal microscopy.

Flow Cytometry. Lung cells were isolated as previously described (44). Single-cell suspensions were prepared using 40-μm cell strainers (BD Biosciences) and treated with antibody mixtures (Table S2) on ice for 30 min. The cells were washed with PBS containing 2% FBS and sorted using a FACSAria (BD Biosciences), and the data were analyzed using FlowJo software (Tree Star).

In Vivo Migration Assay for Inflammatory Monocytes. Mice were administered 200 ng of recombinant mouse CCL2 (PeproTech) intraperitoneally. Six hours later, the mice were killed and injected intraperitoneally with 5 mL of PBS containing 2% FBS. Peritoneal fluid was subsequently collected and analyzed by flow cytometry. For glycolytic inhibition assays, 0.5 g/kg b.w. of 2-DG was administered intraperitoneally 1 h before CCL2 treatment.

Measurement of ATP. ATP levels were normalized to total protein concentration, as determined using a Bradford assay kit (Bio-Rad) as previously described (57).

Statistical Analyses. Statistical analyses were performed using GraphPad Prism software. The Mann–Whitney *U*, Student's *t*, and Fisher's exact tests were used for statistical evaluations. Log-rank tests were used to evaluate statistical differences in Kaplan–Meier analyses. Data are represented as mean ± SEM or mean ± SD; P values <0.05 were considered to be significant.

Detailed materials and methods are included in *SI Materials and Methods*.

ACKNOWLEDGMENTS. We thank Naohiko Koshikawa and Hiroaki Taniguchi for helpful discussions, and Seiko Yoshino, Jane S. Weng, Yuka Takahashi, and Miho Ishiura for technical support. This work was supported by a Grant-in-Aid for JSPS Fellows from the Japan Society for the Promotion of Science (to T. Hara), Grant-in-Aid for Scientific Research (S) and on Priority Areas, Integrative Research toward the Conquest of Cancer, from MEXT (to M.S.), and Grant-in-Aid for Scientific Research (C), Grant-in-Aid for Scientific Research on Innovative Areas, and P-DIRECT (Project for Development of Innovative Research on Cancer Therapeutics) and P-CREATE (Project for Cancer Research and Therapeutic Evolution) grants from the Japan Agency for Medical Research and Development (to T.S.).

1. Chiang AC, Massagué J (2008) Molecular basis of metastasis. *N Engl J Med* 359: 2814–2823.
2. Valastyan S, Weinberg RA (2011) Tumor metastasis: Molecular insights and evolving paradigms. *Cell* 147:275–292.
3. Chen Q, Zhang XH, Massagué J (2011) Macrophage binding to receptor VCAM-1 transmits survival signals in breast cancer cells that invade the lungs. *Cancer Cell* 20: 538–549.
4. Granot Z, et al. (2011) Tumor entrained neutrophils inhibit seeding in the premetastatic lung. *Cancer Cell* 20:300–314.
5. Labelle M, Begum S, Hynes RO (2011) Direct signaling between platelets and cancer cells induces an epithelial-mesenchymal-like transition and promotes metastasis. *Cancer Cell* 20:576–590.
6. De Palma M, Lewis CE (2013) Macrophage regulation of tumor responses to anticancer therapies. *Cancer Cell* 23:277–286.
7. Mantovani A, Allavena P, Sica A, Balkwill F (2008) Cancer-related inflammation. *Nature* 454:436–444.
8. Qian BZ, Pollard JW (2010) Macrophage diversity enhances tumor progression and metastasis. *Cell* 141:39–51.
9. Cortez-Retamozo V, et al. (2013) Angiotensin II drives the production of tumor-promoting macrophages. *Immunity* 38:296–308.
10. DeNardo DG, et al. (2011) Leukocyte complexity predicts breast cancer survival and functionally regulates response to chemotherapy. *Cancer Discov* 1:54–67.
11. Geissmann F, et al. (2010) Development of monocytes, macrophages, and dendritic cells. *Science* 327:656–661.
12. Charo IF, Ransohoff RM (2006) The many roles of chemokines and chemokine receptors in inflammation. *N Engl J Med* 354:610–621.
13. Serbina NV, Pamer EG (2006) Monocyte emigration from bone marrow during bacterial infection requires signals mediated by chemokine receptor CCR2. *Nat Immunol* 7:311–317.
14. Qian BZ, et al. (2011) CCL2 recruits inflammatory monocytes to facilitate breast-tumour metastasis. *Nature* 475:222–225.
15. Zhang Y, et al. (2013) miR-126 and miR-126* repress recruitment of mesenchymal stem cells and inflammatory monocytes to inhibit breast cancer metastasis. *Nat Cell Biol* 15:284–294.
16. Sanford DE, et al. (2013) Inflammatory monocyte mobilization decreases patient survival in pancreatic cancer: A role for targeting the CCL2/CCR2 axis. *Clin Cancer Res* 19:3404–3415.
17. Cramer T, et al. (2003) HIF-1alpha is essential for myeloid cell-mediated inflammation. *Cell* 112:645–657.
18. Kaelin WG, Jr, Ratcliffe PJ (2008) Oxygen sensing by metazoans: The central role of the HIF hydroxylase pathway. *Mol Cell* 30:393–402.
19. Semenza GL (2010) HIF-1: Upstream and downstream of cancer metabolism. *Curr Opin Genet Dev* 20:51–56.
20. Hara T, et al. (2011) Deletion of the Mint3/Apba3 gene in mice abrogates macrophage functions and increases resistance to lipopolysaccharide-induced septic shock. *J Biol Chem* 286:32542–32551.
21. Sakamoto T, Seiki M (2009) Mint3 enhances the activity of hypoxia-inducible factor-1 (HIF-1) in macrophages by suppressing the activity of factor inhibiting HIF-1. *J Biol Chem* 284:30350–30359.
22. Hara T, Mimura K, Seiki M, Sakamoto T (2011) Genetic dissection of proteolytic and non-proteolytic contributions of MT1-MMP to macrophage invasion. *Biochem Biophys Res Commun* 413:277–281.
23. Padua D, et al. (2008) TGFbeta primes breast tumors for lung metastasis seeding through angiopoietin-like 4. *Cell* 133:66–77.
24. Tsai JH, Donaher JL, Murphy DA, Chau S, Yang J (2012) Spatiotemporal regulation of epithelial-mesenchymal transition is essential for squamous cell carcinoma metastasis. *Cancer Cell* 22:725–736.
25. Qian B, et al. (2009) A distinct macrophage population mediates metastatic breast cancer cell extravasation, establishment and growth. *PLoS One* 4:e6562.
26. Auguste P, et al. (2007) The host inflammatory response promotes liver metastasis by increasing tumor cell arrest and extravasation. *Am J Pathol* 170:1781–1792.
27. Khatib AM, et al. (2005) Characterization of the host proinflammatory response to tumor cells during the initial stages of liver metastasis. *Am J Pathol* 167:749–759.
28. Kneuer C, Ehrhardt C, Radomski MW, Bakowsky U (2006) Selectins—Potential pharmacological targets? *Drug Discov Today* 11:1034–1040.
29. Keith B, Johnson RS, Simon MC (2011) HIF1α and HIF2α: Sibling rivalry in hypoxic tumour growth and progression. *Nat Rev Cancer* 12:9–22.
30. Hiratsuka S, et al. (2011) Endothelial focal adhesion kinase mediates cancer cell homing to discrete regions of the lungs via E-selectin up-regulation. *Proc Natl Acad Sci USA* 108:3725–3730.
31. Kitamoto K, et al. (2009) Effects of liposome clodronate on renal leukocyte populations and renal fibrosis in murine obstructive nephropathy. *J Pharmacol Sci* 111: 285–292.
32. Deng J, et al. (2012) S1PR1-STAT3 signaling is crucial for myeloid cell colonization at future metastatic sites. *Cancer Cell* 21:642–654.
33. Hiratsuka S, et al. (2013) Primary tumours modulate innate immune signalling to create pre-metastatic vascular hyperpermeability foci. *Nat Commun* 4:1853.
34. Peinado H, et al. (2012) Melanoma exosomes educate bone marrow progenitor cells toward a pro-metastatic phenotype through MET. *Nat Med* 18:883–891.
35. Fidler IJ (1973) Selection of successive tumour lines for metastasis. *Nat New Biol* 242: 148–149.
36. Reddy BV, Kalraiya RD (2006) Sialilated β1,6 branched N-oligosaccharides modulate adhesion, chemotaxis and motility of melanoma cells: Effect on invasion and spontaneous metastasis properties. *Biochim Biophys Acta* 1760:1393–1402.
37. Joyce JA, Pollard JW (2009) Microenvironmental regulation of metastasis. *Nat Rev Cancer* 9:239–252.

38. Bracken CP, et al. (2006) Cell-specific regulation of hypoxia-inducible factor (HIF)-1alpha and HIF-2alpha stabilization and transactivation in a graded oxygen environment. *J Biol Chem* 281:22575–22585.
39. Sakamoto T, Seiki M (2010) A membrane protease regulates energy production in macrophages by activating hypoxia-inducible factor-1 via a non-proteolytic mechanism. *J Biol Chem* 285:29951–29964.
40. Ren G, et al. (2012) CCR2-dependent recruitment of macrophages by tumor-educated mesenchymal stromal cells promotes tumor development and is mimicked by TNFα. *Cell Stem Cell* 11:812–824.
41. van Deventer HW, Palmieri DA, Wu QP, McCook EC, Serody JS (2013) Circulating fibrocytes prepare the lung for cancer metastasis by recruiting Ly-6C+ monocytes via CCL2. *J Immunol* 190:4861–4867.
42. Hong KH, Ryu J, Han KH (2005) Monocyte chemoattractant protein-1-induced angiogenesis is mediated by vascular endothelial growth factor-A. *Blood* 105: 1405–1407.
43. Morrison AR, et al. (2014) Chemokine-coupled β2 integrin-induced macrophage Rac2-Myosin IIA interaction regulates VEGF-A mRNA stability and arteriogenesis. *J Exp Med* 211:1957–1968.
44. Wolf MJ, et al. (2012) Endothelial CCR2 signaling induced by colon carcinoma cells enables extravasation via the JAK2-Stat5 and p38MAPK pathway. *Cancer Cell* 22:91–105.
45. Liu Y, Cao X (2016) Characteristics and significance of the pre-metastatic niche. *Cancer Cell* 30:668–681.
46. Auffray C, et al. (2007) Monitoring of blood vessels and tissues by a population of monocytes with patrolling behavior. *Science* 317:666–670.
47. Ehling J, et al. (2014) CCL2-dependent infiltrating macrophages promote angiogenesis in progressive liver fibrosis. *Gut* 63:1960–1971.
48. Dunay IR, et al. (2008) Gr1(+) inflammatory monocytes are required for mucosal resistance to the pathogen *Toxoplasma gondii*. *Immunity* 29:306–317.
49. León B, López-Bravo M, Ardavín C (2007) Monocyte-derived dendritic cells formed at the infection site control the induction of protective T helper 1 responses against *Leishmania*. *Immunity* 26:519–531.
50. Claassen E, Van Rooijen N (1984) The effect of elimination of macrophages on the tissue distribution of liposomes containing [^{3}H]methotrexate. *Biochim Biophys Acta* 802:428–434.
51. Headley MB, et al. (2016) Visualization of immediate immune responses to pioneer metastatic cells in the lung. *Nature* 531:513–517.
52. Barthel SR, Gavino JD, Descheny L, Dimitroff CJ (2007) Targeting selectins and selectin ligands in inflammation and cancer. *Expert Opin Ther Targets* 11:1473–1491.
53. Winkler IG, et al. (2012) Vascular niche E-selectin regulates hematopoietic stem cell dormancy, self renewal and chemoresistance. *Nat Med* 18:1651–1657.
54. Clausen BE, Burkhardt C, Reith W, Renkawitz R, Förster I (1999) Conditional gene targeting in macrophages and granulocytes using LysMcre mice. *Transgenic Res* 8: 265–277.
55. Hoshino D, Koshikawa N, Seiki M (2011) A p27(kip1)-binding protein, p27RF-Rho, promotes cancer metastasis via activation of RhoA and RhoC. *J Biol Chem* 286: 3139–3148.
56. Yoshino S, et al. (2012) Genetic screening of new genes responsible for cellular adaptation to hypoxia using a genome-wide shRNA library. *PLoS One* 7:e35590.
57. Sakamoto T, Niiya D, Seiki M (2011) Targeting the Warburg effect that arises in tumor cells expressing membrane type-1 matrix metalloproteinase. *J Biol Chem* 286: 14691–14704.